A98-31547

ICAS-98-3,4,5

CONSIDERATIONS IN APPLYING MILITARY AIRCRAFT FOREBODY FLOW CONTROL METHODOLOGY TO COMMERCIAL AIRCRAFT

Martin E. Beyers#
Institute for Aerospace Research
Ottawa, Ontario, Canada K1A 0R6

Lars E. Ericsson *
Mountain View, California 94040

Abstract

The implications of applying forebody flow control technology to a high-speed civil transport (HSCT) configuration are analyzed. Unlike the case of combat aircraft, where the effective range for forebody flow control is in the post-stall regime, for the HSCT the control is required at the moderate angles of attack of take-off and landing, where additional flow parameters become important. The main complication in transferring the technology to civil aircraft is the large difference in forebody slenderness, with apex half-angles below 10 deg compared to above 25 deg for military aircraft. Available experimental results for aircraft are interpreted using the existing data base for bodies of revolution. Lateral-directional control requirements for an HSCT in the low-speed flight phase are considered.

Nomenclature

b	wing span
c	reference length, c = D
D	maximum body diameter
l_N	nose length
$\dot{m}$	blowing mass flow rate, coefficient $C_\mu = \dot{m}/q_\infty S$
M	Mach number
N	normal force, coefficient $C_N = N/q_\infty S$; $c_n = \partial C_N/\partial\xi$
n	yawing moment, coefficient $C_n = n/q_\infty Sb$
q_∞	dynamic pressure, $= \rho_\infty U_\infty^2/2$
r	local body radius
Re	Reynolds number, usually $Re = U_\infty c/\nu_\infty$
S	reference area, = projected wing area, $= \pi D^2/4$ for body alone
t	time
t^*	nondimensional time, $= x \tan\alpha/r$
U_∞	freestream velocity
x	axial distance from the nose, of forward edge of slot
Y	side force, coefficient $C_Y = Y/q_\infty S$; $c_y = \partial C_Y/\partial\xi$
α	angle of attack
θ	direction angle of blowing (Fig. 4)
θ_A	apex half angle
ν	kinematic viscosity of air
ξ	dimensionless x-coordinate, $\xi = x/c$
σ	total angle of attack, Eq. (1)
ρ	density of air
ϕ	azimuth angle of blowing port (Fig. 4)
ϕ_m	rotation of stagnation point, Eq. (2)

Subscripts

A	apex
LE	slot leading edge
TE	slot trailing edge
∞	freestream conditions

Introduction

The requirement for acceptable low-speed handling qualities imposes challenging design constraints on aircraft configurations optimized for high-speed cruise. The effectiveness of the vertical and horizontal tails on a high-speed civil transport (HSCT) is reduced at take-off and landing angles of attack, when the tail is immersed in the wing / body wake. With their potential for yaw control demonstrated on fighter aircraft at high alpha[1], it is natural to consider the application of forebody flow control concepts to augment the control of the HSCT at these conditions.

Recently, pneumatic forebody flow control tests were performed at low alpha on a 3%-scale model of the Boeing

Head Aircraft Aerodynamics, Aerodynamics Laboratory
* Engineering Consultant

21st ICAS Congress
13-18 September 1998
Melbourne, Australia

1804 SST configuration[2, 3] (Fig. 1) and on a 6%-scale model of the F-16 forebody. In a subsequent analysis of these results[4] it was found that the technology transfer is complicated by the effects of configurational differences which introduce dependencies on additional parameters in the case of the civil aircraft configuration.

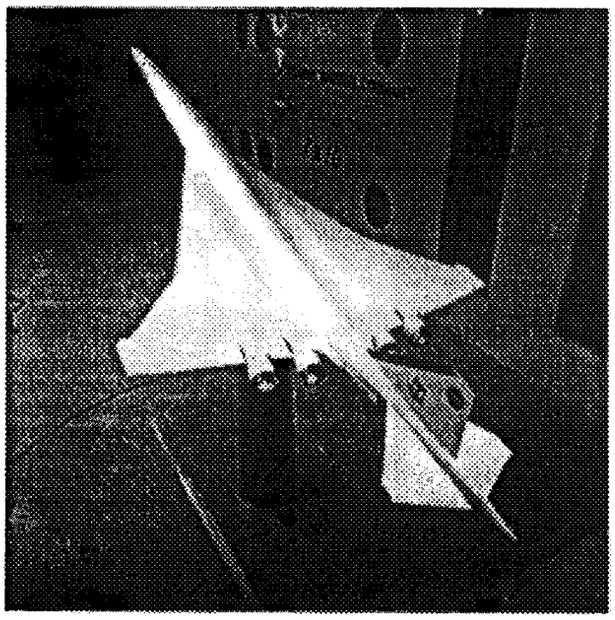

Fig. 1 The 3% scale model of the Boeing 1804 SST aircraft.[2]

In the present paper, the available data are analyzed in greater detail to pinpoint the changes in the forebody control method that are needed in order to obtain the desired control characteristics for commercial aircraft with their very slender forebodies.

General Considerations

Effects of Nose Slenderness

During the approach and landing phase the SST is expected to operate at angles of attack of 10 to 12 deg[2]. In the take-off phase the total angle of attack could be even higher; at rotation, in the presence of a crosswind, giving 5 deg sideslip,

$$\sigma = \cos^{-1}(\cos\alpha \cos\beta) \cong 13 \text{ deg} \qquad (1)$$

To consider the effectiveness of forebody flow control devices on a combat aircraft at these angles of attack, the investigation on a 6% scale model of the F-16 forebody[5] is of interest (Fig. 2). The tests were performed at $0 \le \alpha \le 18°$, $M = 0.8$, and $Re \cong 0.85 \times 10^6$ based on the maximum body-diameter dimension. According to an analysis[6] of data on bodies of revolution[7] the results can be compared with the low-speed SST data [2,3] at $\alpha \le 18$ deg as there are no appreciable compressibility effects on the crossflow

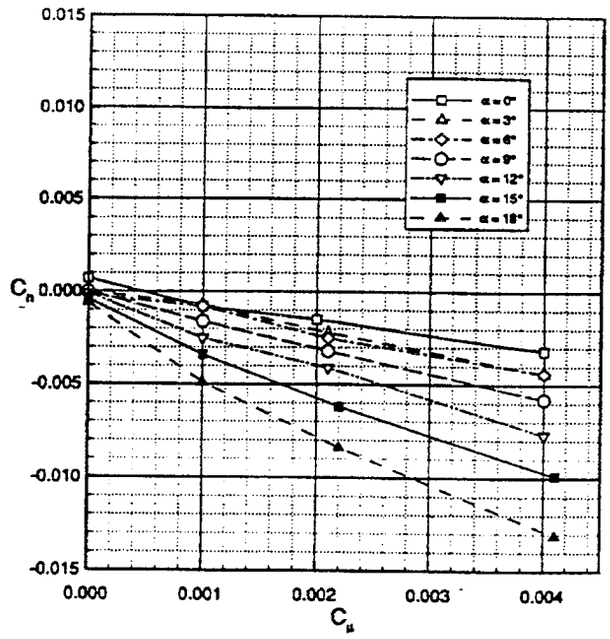

Fig. 2 Pneumatic vortex control at M = 0.8 on a 6% scale model of the F-16 forebody.[5]

separation characteristics for $M_\infty \sin\alpha \le 0.4$. Linear dependence of C_n on the blowing rate was obtained, but the maximum response was equivalent to only a 6.5 deg rudder deflection on the complete aircraft[5]. This is to be expected as $\theta_A > 25°$, $\alpha/\theta_A < 1$, where the forebody crossflow is attached and control capacity is limited by the side force that can be generated by tilting the boundary layer displacement surface.

In contrast, when a similar blowing geometry was applied to the SST aircraft model[2] the nearly linear characteristics observed at $\alpha = 4°$, gave way to highly nonlinear behaviour when the angle of attack was increased to $\alpha = 12°$ (Fig. 3). The Boeing 1804 SST configuration has a proprietary forebody geometry[2], but it is known that

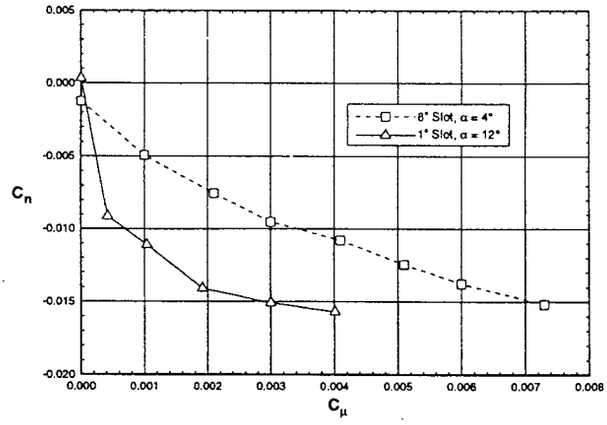

Fig. 3 Effect of asymmetric blowing on SST model at $\alpha = 4$ and 12 deg.[2]

the forebody fineness ratio is 7 and the nose half-angle is in the range of 9 to 10 deg. For the purposes of this discussion it is assumed that $\theta_A = 10$ deg. Thus, at $\alpha = 4°$, $\alpha/\theta_A < 0.5$, and the behaviour is expected to be similar to that for the F-16 (Fig. 2). At $\alpha = 12°$, i.e. $\alpha/\theta_A = 1.46$, Fig. 3 shows that initially for $C_\mu \leq 0.0004$, the magnitude of the C_n (C_μ) slope is one order of magnitude larger than at $\alpha = 4°$. The reason is that at $\alpha = 12°$ in Fig. 3, $1 < \alpha/\theta_A < 2$ and symmetric forebody crossflow separation occurs in the absence of blowing [6]. The modest blowing rate $C_\mu = 0.0004$ was enough to cause asymmetric crossflow separation. Once this change from symmetric to asymmetric crossflow separation has taken place, however, the C_n (C_μ) slope for $C_\mu > 0.0004$ is of the same magnitude as for $\alpha = 4°$. The difference in slot length, 8 inches at $\alpha = 4°$ and 1 inch for the $\alpha = 12°$ data could have had some effect. However, the main reason for the observed differences in the characteristics is the absence of, and presence of crossflow separation, respectively.

The effects of slot geometry on the SST forebody are considered in the discussion that follows. The geometry of the tangential blowing slots and nozzles is shown in Fig. 4. One pair of nozzles is located at $\xi = 1.0$, whereas the slot

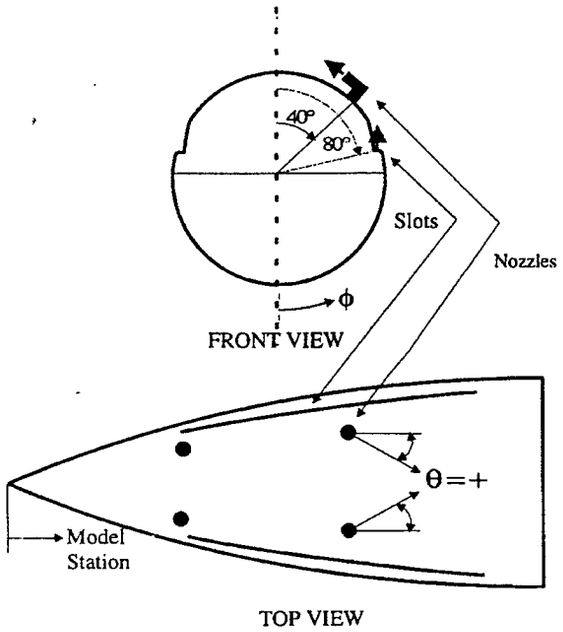

Fig 4. Pneumatic vortex control slot and nozzle orientation on the SST model.[2]

locations are in the range $1.00 \leq \xi \leq 2.7$. Although the present discussion concentrates on the slot blowing results, it is worth noting that slots and nozzles produced different microasymmetry effects[3]. The very large microasymmetry due to nozzles angled at $\theta = 30°$ (Fig. 4), producing a flow separation asymmetry at angles of attack as low as 12° ($\alpha/\theta_A = 1.20$), could be overpowered by a moderate blowing rate[3]. Of greater relevance is the fact that symmetric slot blowing[2] by one-inch slots at a modest blowing rate $C_\mu = 0.0003$ was able to eliminate the effect of slot microasymmetry (Fig. 5).

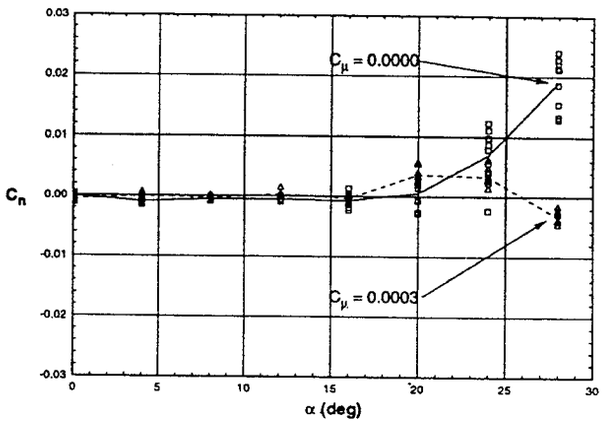

Fig. 5. Effect on $C_n(\alpha)$ of symmetric blowing by the one-inch slot geometry for SST model.[2]

Pneumatic forebody flow control is strongly dependent on the crossflow Reynolds number. The present tests were performed at $Re = 0.51 \times 10^6$ based on the maximum body diameter, and the resulting effects on the control characteristics are analyzed on the basis of the existing data base for bodies of revolution.

Crossflow Separation on Bodies of Revolution

To understand the observed behaviour it is necessary to take the relevant flow physics into account. Surface flow visualization data obtained by Keener[8] on a 3.5-caliber ogive (Fig. 6) were at a higher critical Reynolds number, $Re = 0.8 \times 10^6$, than in the present tests (0.51×10^6), but nevertheless give a good idea of the complexity of the flow field under discussion. Figure 6 shows the development of the three regions of flow separation at this Reynolds number; laminar, transitional and turbulent. A cursory look at these results would be enough to appreciate that the response to slot blowing would be strongly dependent on the location of the slots. Blowing in the turbulent separation region could have relatively little effect upstream, but any disturbance upstream of the transition front affects the evolution of the entire flow field, thereby determining the resulting flow separation characteristics. With an increase in Reynolds number this region shrinks as the transition front moves closer to the apex.

The corresponding effect on the side force distribution is shown in Fig. 7 for an ogive cylinder at $\alpha = 50$ deg through the critical Reynolds number range[9]. Increasing the supercritical Reynolds number starts the side force development progressively closer to the nose-tip, resulting in

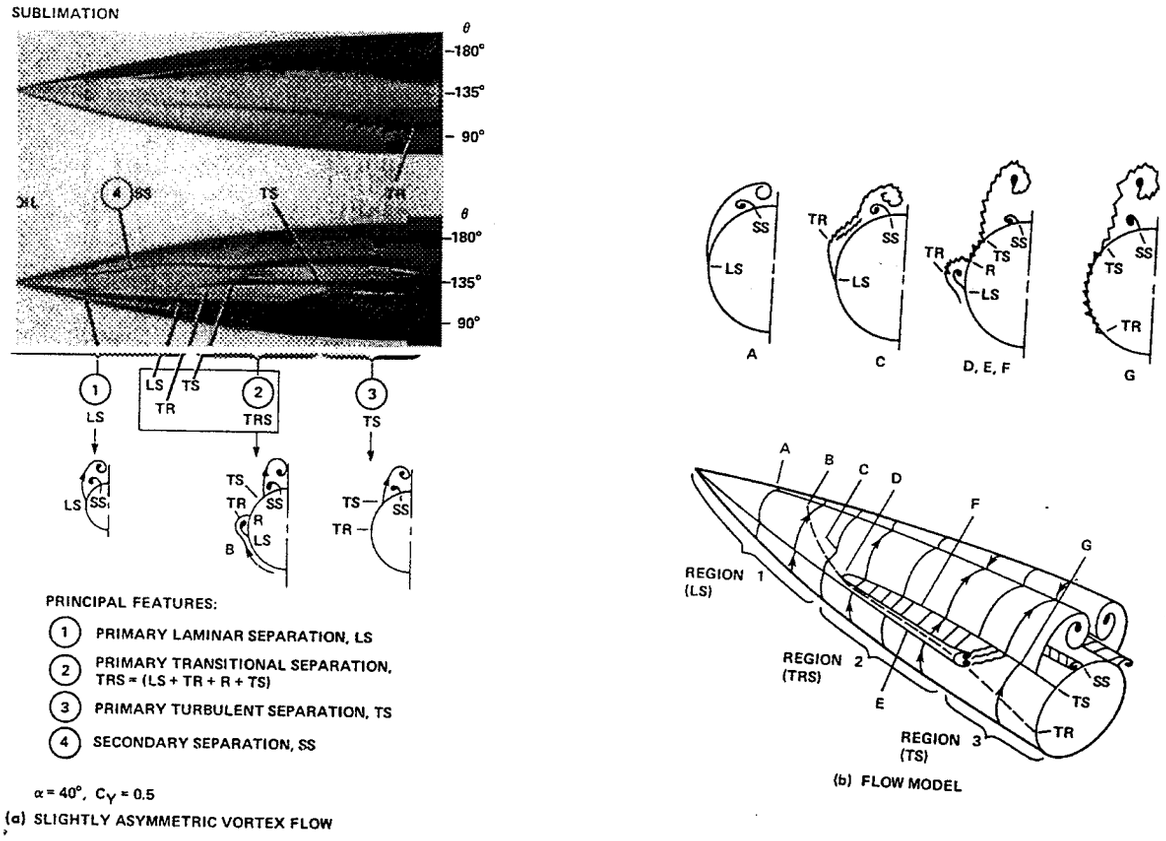

Fig. 6 Flow pattern for 3.5-caliber ogive at M = 0.25, Re = 0.8 x 10^6 (Ref. 8).

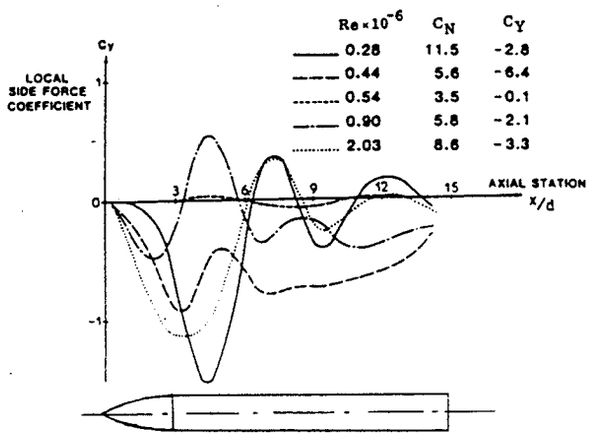

Fig. 7 Side force distribution at α = 50° on an ogive-cylinder through the critical Reynolds number range.[9]

a multi-cellular loading distribution. These results illustrate the great Re - sensitivity of the crossflow separation in the critical range. As in the case of a circular cylinder in crossflow (Fig. 8) conditions for both maximum and minimum side force occur in the critical range[6]. At Re = 0.51 x 10^6 the crossflow conditions on the SST model were in the critical range and apparently established the minimum side force. This would explain how symmetric blowing at a very low rate, C_μ = 0.0003, could have eliminated the yawing moment due to microasymmetry (Fig. 5).

At a constant Reynolds number an increase in α will also cause the side force to be generated progressively closer to the nose apex, and result in a multi-cellular distribution. This is confirmed by the local side-force distribution for an l_N/D = 3.5 tangent ogive cylinder[10] at Re = 0.2 x 10^6 in Fig. 9. The results collapsed on one curve when applying the impulsive flow analogy for slender bodies[11]. Thus, the ogive-cylinder data can be applied directly to the SST model, after accounting for the similarity parameters Re and α/θ_c in determining the loading distribution.

Forebody Slot Blowing on SST Model

The experimental results[2] in Fig. 10 show the sensitivity to α of the effect of asymmetric blowing by a one-inch slot at ξ = 1.0, and reveal that for C_μ = 0.0040 control reversal occurs at α > 10°. It is known that through its effect on the boundary layer, blowing can affect flow separation in a manner similar to the effects of changing the Reynolds number. Thus, when the blowing rate was increased from

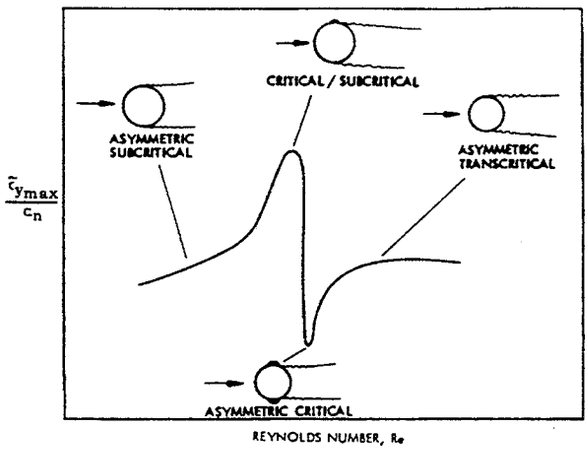

Fig. 8 Expected effects of flow-separation type on the normalized side force.[6]

$C_\mu = 0.0003$ to $C_\mu = 0.0040$ in Fig. 10, the response would be expected to be somewhat equivalent to the effect of increasing the supercritical Reynolds number, perhaps corresponding to the change from $Re = 0.44 \times 10^6$ to $Re = 0.90 \times 10^6$ in Fig. 7. A dramatic redistribution of the loading on the forebody would result, as was seen in the reversal of the slope $C_{n\alpha}$ near $\alpha = 10$ deg or $\alpha/\theta_A \cong 1$. To shed more light on the nature of these results, the effects of changing slot orientation are considered.

At $\alpha/\theta_A > 1$ the blowing controls the separation asymmetry. As noted earlier, an increase in Reynolds number would move the supercritical separation closer to the nose tip. Conversely, moving the blowing slot aft at a fixed Reynolds number would, in general, increase the length of the first asymmetric cell, with an effect similar to that of decreasing the Reynolds number in Fig. 7, for instance, from $Re = 0.90 \times 10^6$ to $Re = 0.44 \times 10^6$. Thus, the experimental results in Fig. 7 for the effect of Reynolds number on the side force distribution on bodies of revolution qualitatively illustrate the potential effect of changing the slot location for blowing at critical crossflow conditions on the SST model.

The results in Figs. 11 and 12 show the effect of axial location of the slots for $C_\mu = 0.0040$ blowing on the left (port) side[3]. Slot configurations were designated by the slot length and location, e.g. 2/4 is a 2 inch slot 4 inches aft of the most forward location possible, $\xi_{LE} = 1.0$, or 5.5 inches aft of the nose apex[3] (D = 5.5 inches). The most aft location of the slot trailing edge was $\xi_{TE} = 2.7$. In interpreting the SST responses to slot blowing one notices that the effect of moving the slot aft is insignificant until the angle of attack reaches $\alpha = 12$ deg $\cong 1.2\theta_A$. The yawing moment generated changes sign, $C_n > 0$, near $\alpha = 16$ deg $> 1.5\theta_A$, at the most forward locations, 1/0 and 2/0, where the slot leading edge is at $\xi_{LE} = 1.0$. These data are nearly identical, confirming that ξ_{LE} is a key parameter. Aft of a certain location the results

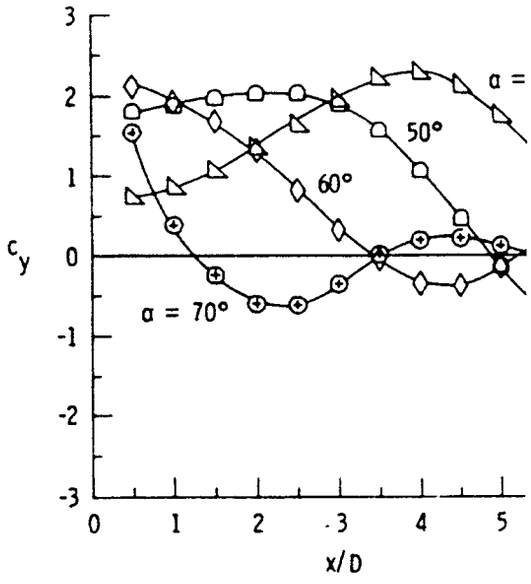

(a) As a function of axial position

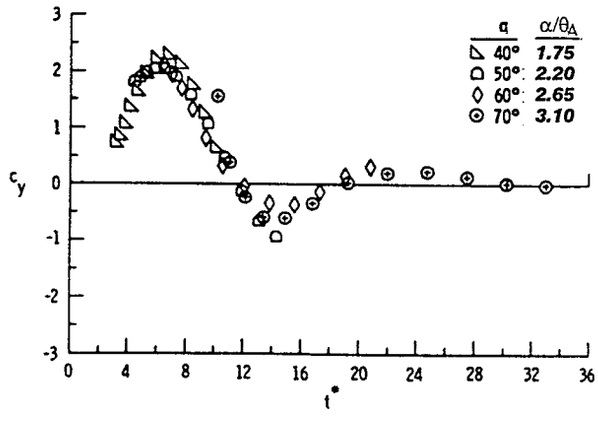

(b) As a function of nondimensional time

Fig. 9 Local side force distribution for $l_N/D = 3.5$ tangent-ogive cylinder at $Re = 0.2 \times 10^6$ (Ref. 10).

are again very similar; e.g. 1/3 and 2/2. In both cases, $\xi_{TE} = 1.73$, indicating that for the aft slot locations, the location of the trailing edge is the important parameter.

One possible explanation of these results is that the first cell of separation on the unblown forebody, corresponding to the laminar region in Fig. 6, is affected only by blowing in the forward locations, near $\xi = 1.0$, whereas in the aft locations the blowing expands the turbulent separation region. To test this hypothesis, it should be remembered that critical conditions exist on the unblown SST forebody, and it is very likely that at the test Reynolds number, $Re = 0.51 \times 10^6$, the minimum side force is established at high α, judging by the results at $\alpha/\theta_A \cong 2$ in Fig. 7.

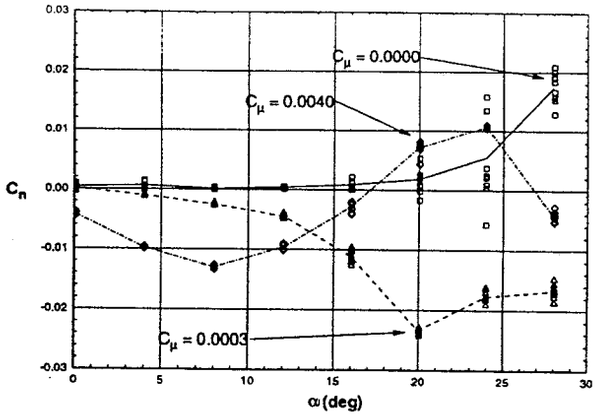

Fig. 10 Sensitivity to angle of attack of the effect of asymmetric blowing by one inch slot at $\xi_{LE} = 1.0$ on SST model.[2]

The blowing slots are located at an azimuth of $\phi_m = 100$ deg (Fig. 4). This means that blowing in the laminar region near the apex would simply add momentum to the flow already separated at $\phi \cong 80$ deg, through its wall-jet-like effect on the boundary layer. The axial component of the jet would tend to prevent reattachment of the separated shear layer further downstream in the initially transitional region (Fig. 6). On the unblown (starboard) side, the reattachment and subsequent secondary separation in the transitional region is unaffected, creating a separation asymmetry similar to the subcritical / critical condition in Fig. 8. This produces a positive side force on a section of the forebody, resulting in $C_n > 0$ at high α as seen in Figs. 11 and 12.

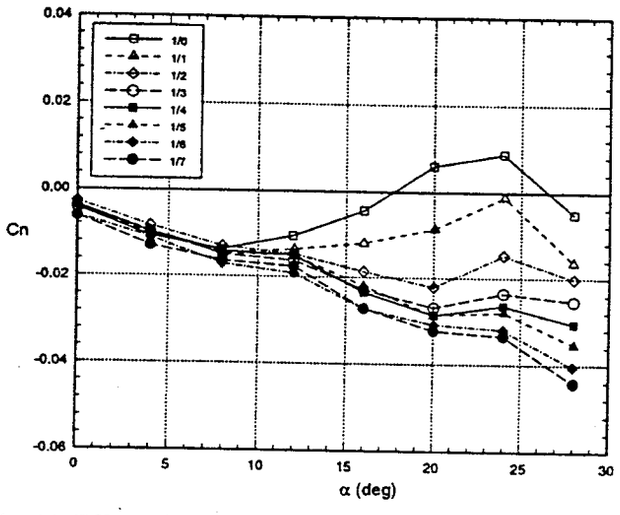

Fig. 11 Effect of axial location of one inch slot on the effect of $C_\mu = 0.0040$ blowing.[3]

In contrast, for slots located further aft, $\xi_{TE} > 1.5$, the blowing effect on the boundary layer apparently expands the second cell of separation, resulting in turbulent separation (Fig. 6) over much of the forebody. The increased length of the main cell of separation on the blown (port) side should result in $C_n < 0$. This is corroborated by the results in Figs. 11 and 12, which show identical $C_n(\alpha)$ characteristics

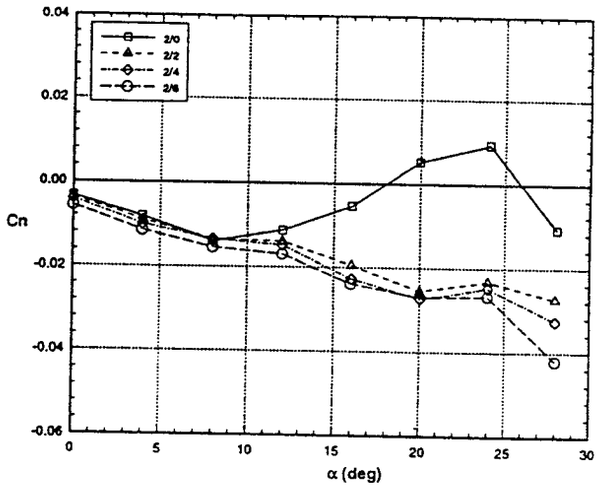

Fig. 12. Effect of axial location of two inch slot on the effect of $C_\mu = 0.0040$ blowing.[3]

for slots with the same location ξ_{TE}; compare, for instance, slots 1/7 with 2/6, or 1/5 with 2/4, in Figs. 11 and 12, respectively.

In the presence of sideslip the effectiveness of forebody pneumatic flow control will be a function of the rotation of the stagnation point.

$$\phi_m = \tan^{-1} (\tan \beta / \sin \alpha) \qquad (2)$$

At typical take-off and landing conditions, $\alpha = 12$ deg and $\beta = 5$ deg, Eq. (2) gives $\phi_m = 22.8$ deg. Thus, the windward slot is located at 77 deg and the leeward slot at 123 deg. Near the apex, $\xi_{LE} \leq 1$, the laminar separation on the unblown forebody is located at $\phi \cong 80$ deg and the response to slot blowing can be expected to exhibit a highly nonlinear dependence on sideslip. However, this could not be confirmed for lack of either slot- or nozzle-blowing data at these conditions.

Results obtained at $\alpha = 12$ deg for an aft slot location, 1/7 (Fig. 13), confirm that slot blowing effectiveness is a function of β. In this case the blowing acts on the supercritical separation cell, where $\phi \cong 105$ deg. On the windward side the blowing always occurs before the separation point on the unblown forebody, while for the leeward side it is normally aft of the unblown separation point. Thus, the pneumatic control is expected to be relatively well-behaved. Nevertheless, Fig. 13 shows that for $\beta < 0$, where the blowing was on the leeward side, $C_{n\beta} \cong 0$ for moderate blowing rates, $C_\mu \leq 0.0010$, so that the blown configuration has become marginally stable, compared to the

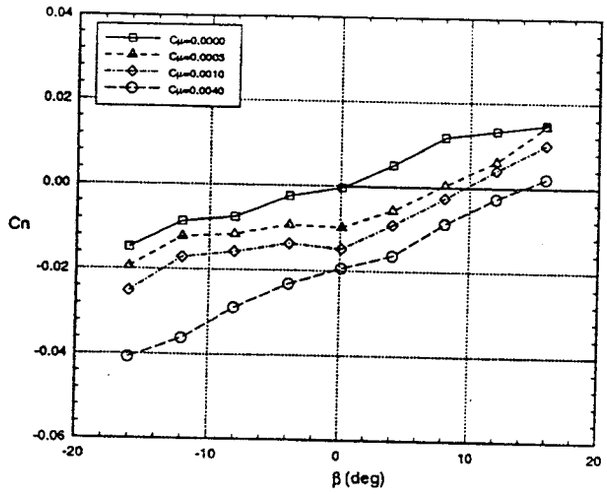

Fig. 13. Effect of sideslip on blowing with 1/7 slot configuration at $\alpha = 12°$ (Ref. 3).

statically stable unblown case. At the maximum blowing rate $C_\mu = 0.0040$ the blowing is fully effective. These trends become more pronounced as α is increased and at $\alpha \geq 16°$ the response is nonlinear at all blowing rates (Fig. 14).

Forebody Flow Control during Take-Off and Landing

At take-off conditions there are conflicting requirements for forebody flow control. During acceleration up to rotation the crossflow Reynolds numbers are low and blowing near

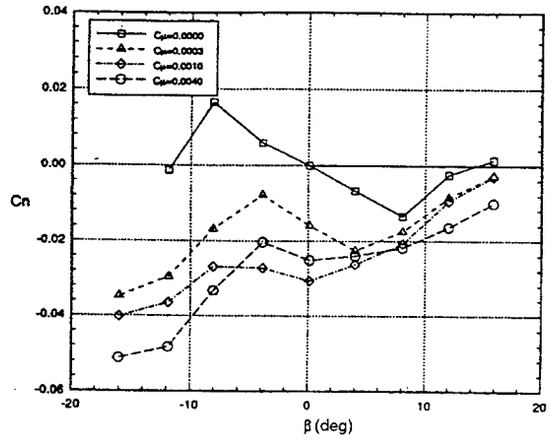

Fig. 14. Effect of sideslip on blowing with 1/7 slot configuration at $\alpha = 20°$ (Ref. 3).

the nose apex would be most effective. On the other hand, in the presence of strong crosswinds appreciable sideslip angles may be present, $0° < \beta < 10°$, and aft blowing locations are most effective. The solution might be to provide additional slots at a larger azimuthal angle ϕ_m as this would permit simultaneous optimization of the azimuthal and longitudinal locations.

The analysis suggests that effective control could be achieved if slot axial and azimuthal locations were to be continuously adjusted to suit the flight conditions $\alpha(t)$, $\beta(t)$ and Re(t) along the take-off and landing paths.

In addition to this control schedule, proportional control has to be provided by the flow control devices. One approach to this problem, which is necessitated by the bistable nature of the crossflow separation asymmetry, is to control the time duration of the left- and right-hand side separation asymmetries[12]. However, this type of duty cycle control mechanism may not be necessary when a flexible slot blowing control schedule is used, following the logic described above. Simultaneous slot blowing on both sides with independently scheduled slot locations and orientations will provide proportional control without generating the unsteadiness associated with pulsed blowing. Such unsteadiness could have an adverse effect on flow separation in the transitional range.

Conclusions

1. The transfer of forebody flow control technology from military to high-speed civil aircraft is not trivial.

2. The observed responses of an SST model to forebody blowing can be explained on the basis of existing knowledge of high-alpha flows.

3. Satisfactory control of take-off and landing maneuvers of an HSCT through the use of forebody flow control devices would require full control of blowing location and orientation, as well as simultaneous independent left- and right-hand side flow control.

References

[1] Malcolm, G. N.,"Forebody Vortex Control - A Progress Review," AIAA Paper 93-3540, Aug. 1993.

[2] Takahashi, T. T., Eidson, R. C., and Heineck, J.T., "Aerodynamic Characteristics of a Supersonic Transport with Pneumatic Flow Control," AIAA Paper 97-0043, Jan. 1997.

[3] Parker, B. A., Eidson, R. C., and Takahashi, T. T., "Forebody Vortex Flow Control on a High Speed Transport Configuration," AIAA Paper 97-0044, Jan. 1997.

[4] Ericsson, L. E., and Beyers, M. E., "Effect of Nose Slenderness on Forebody Flow Control," AIAA Paper 98-0499, Jan. 1998.

[5] Eidson, R. C., and Mosbarger, N. A., "Forebody Pneumatic Devices at Low Angles of Attack and Transonic Speed," AIAA Paper 97-0042, Jan. 1997.

[6] Ericsson, L. E. and Reding, J. P., "Asymmetric Flow Separation and Vortex Shedding on Bodies of Revolution," Chapter 10, Tactical Missile Aerodynamics, General Topics, Vol. 141, Progress Astro. and Aero. series, M.J. Hemsch editor, 1992, pp. 391-452.

[7] Wardlaw, A. B. Jr. and Morrison, A. M., " Induced Side Forces at High Angles of Attack," Naval Surface Warfare Center/WOL, TR-75-176, Nov. 1975

[8] Keener, E. R., "Flow-Separation Patterns on Symmetric Forebodies," NASA TM-86016, Jan. 1986.

[9] Champigny, P., "Reynolds Number Effect on the Aerodynamic Characteristics of an Ogive-Cylinder at High Angles of Attack," AIAA Paper 84-2176, Aug. 1984.

[10] Hall, R. M., "Forebody and Missile Side Forces and the Time Analogy," AIAA Paper 87-0327, Jan. 1987.

[11] Sarpkaya, T., "Separated Flow About Lifting Bodies and Impulsive Flow About Cylinders," AIAA Journal, Vol. 4, No. 3, 1966, pp. 414-420.

[12] Lee, R., Hanff, E. S., and Kind, R. J., " Linear Control of Side Forces and Yawing Moments Using the Dynamic Manipulation of Forebody Vortices," ICAS 96-2.10.1, Sept. 1996.